

The role of microstructure in luminescent properties of Er-doped nanocrystalline Si thin films

© M.V. Stepikhova, M.F. Cerqueira*, M. Losurdo**, M.M. Giangregorio**, E. Alves***, T. Monteiro****, M.J. Soares****

Institute for Physics of Microstructures, Russian Academy of Sciences, 603950 Nizhnii Novgorod, Russia

* Departamento de Física, Universidade do Minho, Campus de Gualtar 4710-057 Braga, Portugal

** Institute of Inorganic Methodologies and of Plasmas, IMIP-CNR, via Orabona, 4-70126 Bari, Italy

*** Instituto Técnico Nuclear ITN, EN 10, 2686-953 Sacavém, Portugal

**** Departamento de Física, Universidade de Aveiro, Campus de Santiago 3700 Aveiro, Portugal

In this contribution we present the structural and photoluminescence (PL) analysis of Er doped nanocrystalline silicon thin films produced by rf magnetron sputtering method. We show the strong influence of the presence of nanocrystalline fraction in films on their luminescence efficiency at $1.54\ \mu\text{m}$ that has been studied on the series of specially prepared samples with the different crystallinity, i.e. percentage and sizes of Si nanocrystals. It has been observed the strong, by about two orders of magnitude, increase of Er-related PL intensity in these samples with the lowering of Si nanocrystal sizes from 7.9 to about 1.5 nm. The results are discussed in terms of the sensitization effect of Si nanocrystals on Er ions.

This work was partially supported by FCT foundation (Portugal) and Russian foundation for basic research (RFBR project N 01-02-16439).

1. Introduction

Recently, Er-doped Si materials were widely studied in context with the interest in temperature-stable light emitters for optical communication systems. The intra-4f-shell transitions between two lowest spin-orbit levels of Er^{3+} ions, namely the transitions ${}^4I_{13/2} \rightarrow {}^4I_{15/2}$, occur at $1.54\ \mu\text{m}$, a wavelength close to that with minimum loss in silica based optical fibers. It has been reported on the realization of electroluminescence devices on Si:Er basis [1–3]. Nevertheless the main drawback to use a bulk Si crystal as a host for Er^{3+} is the strong temperature quenching of $1.54\ \mu\text{m}$ luminescence. It appears that this situation may be considerably improved by the incorporation of Er ions in nanocrystal containing materials. The idea is based on the bandgap widening of nanometer size Si that consequently has to result in the reducing of thermal quenching for Er luminescence. Moreover, Si nanocrystals that are well known to emit in the visible range (due to the recombination of confined excitons within the nanostructures) may act as the efficient sensitizers for rare earth ions [4,5].

In this contribution we discuss the luminescent properties of Er-doped nanocrystalline silicon thin films (nc-Si:Er) produced by the r.f. reactive magnetron sputtering method. The advantages of these films, when compare with the intensively studied nanocrystal containing SiO_2 structures and *a*-Si:H,O,Er films, is their relatively high conductivity that makes the material attractive for device applications. One can show that the presence of crystalline fraction in thin films results in the increase of films conductivity in several orders of magnitude [6]. Er-doped nc-Si:H films with the well-defined crystallinity and nanocrystal sizes (varied from

1–3 to 8 nm) were deposited and studied in both near IR ($1.54\ \mu\text{m}$) and visible luminescence ranges. The results are discussed in terms of the role of Si nanocrystallites in films luminescent properties.

2. Experimental

Erbium doped nanocrystalline silicon thin films were grown by r.f. magnetron sputtering in an Ar/H₂ atmosphere on the ordinary glass substrates. The procedure applied was similar to that used for the preparation of undoped $\mu\text{c-Si:H}$ films [7], only modified by the introduction of small pieces of metallic erbium to c-Si target for Er doping. The target used was a c-Si of high purity (99.99%). The erbium was placed in a low erosion area on the silicon target, in order to keep the moderate rate of Er impurity. The substrate–target distance was fixed at 55 mm.

Samples with the different structural parameters, i.e., different crystalline fraction and grain sizes were obtained by the varying of experimental parameters (RF power, temperature, Er content and gas mixture composition). In particular, amorphous films (see Er28) were obtained at low hydrogen dilution, i.e., low R_H value (see Table 1). Nanocrystalline samples were grown in a H₂ rich atmosphere, where the role of atomic hydrogen is to etch preferentially the amorphous phase and promote the amorphous-to-crystalline transition. The films growth conditions are listed in Table 1.

The chemical composition of films was determined by the Rutherford backscattering spectroscopy and elastic recoil detection techniques. The structural characterisation

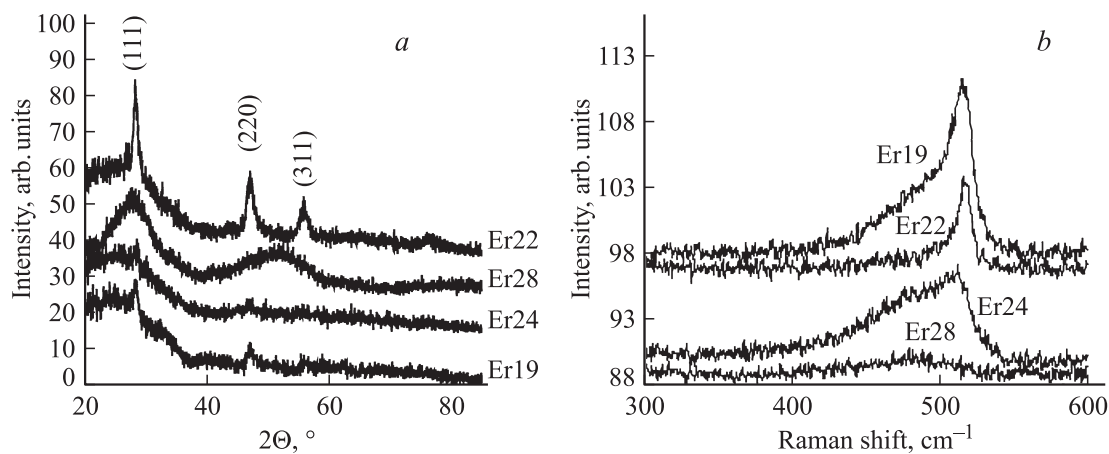


Figure 1. XRD (a) and Raman spectra (b) of nc-Si:Er thin films.

was performed by a standard micro-Raman spectroscopy under excitation with the 514.5 nm Ar⁺-laser line and by X-ray diffractometry in the grazing incidence geometry. For the more detailed analysis of microstructure and films „anatomy“, high-resolution transmission electron microscopy (HRTEM) and spectroscopic ellipsometry (SE) were applied. SE spectra of the pseudodielectric function, $\langle \varepsilon \rangle = \langle \varepsilon_1 \rangle + i\langle \varepsilon_2 \rangle$, were acquired in the 1.5–5.5 eV energy range by using a phase-modulated spectroscopic ellipsometer (UVISEL-Jobin Yvon) at an incident angle of 70.5°. SE spectra were analysed in terms of optical models based on the Bruggeman effective medium approximation (for more details see [8]). The thickness of the films was evaluated from the analysis of interference pattern in transmission spectra making use of the Swanepoel method [9] and from the spectroscopic ellipsometry data. Photoluminescence (PL) measurements in the near IR range have been performed with a Bruker 66 V Fourier-transform spectrometer. The signal was detected with a North-Coast EO-817 liquid nitrogen cooled germanium detector. The 514.5 nm line of an Ar laser was used for the excitation. PL studies in the visible spectral range were carried out under excitation with a 325 nm line of cw He-Cd laser with a Spex 1704 monochromator and cooled Hamamatsu R928 photomultiplier in the detection chain.

Table 1. Growth conditions for erbium doped nanocrystalline silicon thin films

| Sample | Temperature, °C | RF power, W | R_H |
|--------|-----------------|-------------|-------|
| Er22 | 400 | 80 | 0.63 |
| Er19 | 200 | 80 | 0.63 |
| Er24 | 50 | 80 | 0.63 |
| Er28 | 200 | 150 | 0.37 |
| Er33 | 25 | 80 | 0.63 |

$R_H = p_{H_2}/(p_{H_2} + p_{Ar})$ is the hydrogen fraction.

3. Results and discussion

Fig. 1 shows the XRD and Raman spectra for the nc-Si:Er samples studied. The broad band, related to the silicon amorphous matrix, is present in spectra for all samples. The sample Er28 grown at higher RF power but in Ar rich atmosphere does not show any crystalline peak in both the XRD and Raman spectra (the same behaviour was observed also for the sample Er33). In contrast, the (111), (220) and (311) diffraction peaks of c-Si are visible for all other samples. The peaks are well evident for the Er22 sample grown at high H₂ dilution and high temperature of 400°C, both parameters promoting the amorphous-to-crystalline transition. The diffraction peaks have a lower intensity for the Er19 and Er24 samples, indicating a decrease of the crystallinity and/or the crystallites grain sizes that is also confirmed by the intensity ratio of the Stokes peaks at 480 cm⁻¹ (a-Si related) and at 520 cm⁻¹ (transverse optical (TO) mode of c-Si) in Raman spectra (Fig. 1, b). The diffraction peak analysis, by fitting a pseudo-Voigt function to the (111) c-Si diffraction peak [7], gives the average crystal size for Si nanocrystals presented in Table 2. In the same table, there are also the data of Raman spectroscopy. To analyse the Raman spectra, TO replica of amorphous structure has been approximated by a Gaussian profile, and the crystalline response analysis were performed on the basis of Strong Phonon Confinement model [10].

Near IR photoluminescence spectra measured at 77 K in nc-Si:Er samples are shown in Fig. 2. Let consider the highly crystalline samples according to XRD and Raman data (the samples Er24, Er19, Er22 with the nanocrystal sizes of 5.5–7.9 nm and crystallinity $C_R = 23$ –65%). The spectra of these samples show the luminescence peak at 1.54 μm related with the intra-atomic ($^4I_{13/2} \rightarrow ^4I_{15/2}$) transitions of Er³⁺ ions. Being relatively broad in low crystalline sample (sample Er24) with the maximum at 6500 cm⁻¹ and a characteristic shoulder at around 6457 cm⁻¹, like for Er in a glass-like and amorphous materials [11], the Er-related spectrum transforms in highly crystalline films (sample

Table 2. Elements content, thickness and structural parameters of nc-Si:Er samples

| Sample | Er, % | Si, % | O, % | H, % | d , nm | D_X , nm | D_R , nm | C_R , % | SE data |
|--------|-------|-------|------|------|----------|------------|------------|-----------|----------------|
| Er22 | 0.10 | 71.7 | 8.8 | 17.6 | 2089 | 7.0 | 7.9 | 65 | 87% μ c-Si |
| Er19 | 0.12 | 62 | 34 | 23 | 483 | 5.7 | 6.5 | 43 | 31% μ c-Si |
| Er24 | 0.17 | 56.5 | 17.6 | 25.4 | 538 | 3.9 | 5.5 | 23 | 25% μ c-Si |
| Er28 | 0.11 | 60.9 | 2.9 | 34.3 | 1295 | — | — | 0 | 10% nc-Si |
| Er33 | 0.02 | 73.4 | < 1 | 25.8 | 1499 | — | — | 0 | 38% nc-Si |

D — average crystal size, R — Raman spectroscopy, X — XRD analysis, C_R — crystalline volume fraction determined by Raman spectroscopy, d — film thickness.

Er22) in the spectrum with a fine line structure (see the inset *A* in Fig. 2) giving the evidence for the incorporation of Er ions in regular crystalline surroundings. At the same time, in the spectra of highly crystalline samples appear and increase with the crystallinity the lines at 7500 and 9435 cm^{-1} that could be assigned by their energetic position as the defect-like and excitonic transitions in Si crystallites. However, one can see that the increase of crystallinity in these samples results in the strong quenching of Er related photoluminescence. Though the samples have a similar Er atomic percentage (0.1–0.17%, as estimated by RBS), PL intensity in them reduces by more than an order of magnitude with the increasing of crystalline fraction from 23 to 65% (and crystallite sizes from 5.5 to 7.9 nm, see the insert *B* in Fig. 2).

The most intense Er-related PL was observed in low crystalline samples determined as „amorphous“ according to the Raman and XRD analysis (samples Er28 and Er33 in Table 2). In particular, the PL intensity of the sample Er33 exceeds that for highly crystalline sample Er22 by about two orders of magnitude (see the insert in Fig. 2), this is despite the lower Er content. These samples show the strong luminescence at room temperature (Fig. 3). The PL intensity decreases only 5-fold when going from 77 to 300 K with the deactivation energies of 154 and 170 meV.

It seems that it would be difficult to explain this dramatic increase of the luminescent efficiency arising upon the transition from crystalline to amorphous film structure even because of the strong difference in the excitation cross sections for Er ions in these two matrixes. It is known

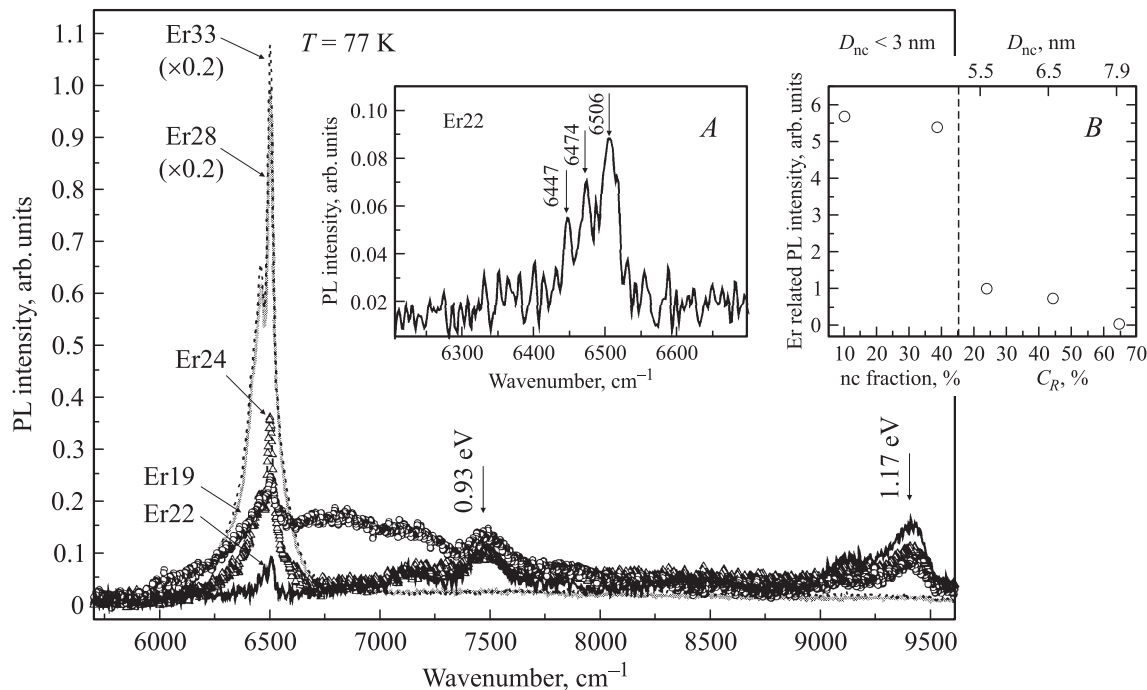


Figure 2. PL spectra of nc-Si:Er samples with the different content of crystalline fraction. Inserts show: *A* — enlarged Er-related region in the PL spectrum for the sample Er22; *B* — correlation between the PL intensity (Er-related peak) and the presence of crystalline fraction in nc-Si:Er samples. Right part of the insert (*B*) shows the situation for highly crystalline samples according to XRD and Raman analysis (the C_R and D_R values on the bottom and top axis correspond to the Raman data). On the left part of the insert (*B*), PL intensities for the samples with the nanocrystallite fraction with 1–3 nm crystallite grain sizes are presented, where the values for nc fraction are taken from SE data. The luminescence intensities at 1.54 μm in this insert are normalised to the films thickness.

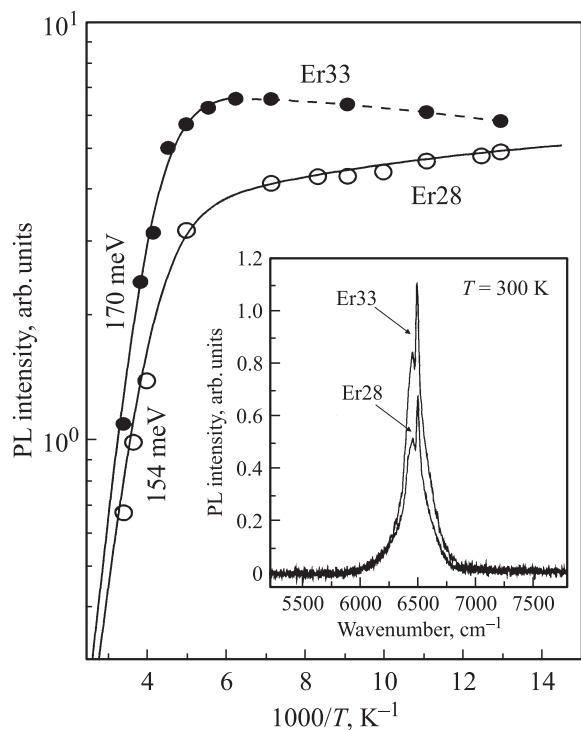


Рис. 3. Temperature dependencies of Er-related PL intensity obtained in nc-Si:Er thin films (samples Er28 and Er33). The solid lines are exponential fits of experimental data with the deactivation energies of 170 and 154 meV, for the samples Er33 and Er28, respectively. The insert shows PL spectra of the samples at room temperature.

that the excitation cross section for the direct excitation of Er ions in amorphous matrixes is by about five orders of magnitude less than that for Er in crystalline Si ($8 \cdot 10^{-21}$ and $3 \cdot 10^{-15} \text{ cm}^2$, respectively [12,13]). Of course, one

cannot exclude the role of nonradiative recombination channels in these composite structures. So, we can image that the enlargement of crystalline fraction will enhance the nanocrystalline interactions in films and therefore the probability for excitons to propagate in crystalline network and recombine nonradiatively. But in fact we didn't observe any direct evidence for the strong influence of nonradiative processes on the films luminescent efficiency. There is no strong correlation between the amount of hydrogen in films and their luminescent properties (as a rule, hydrogen passivates the dangling bonds in amorphous/crystalline tissue thus intensifying PL). Even opposite, we have observed the increase of films PL intensity after annealing at 500°C for 5 hours, a procedure depleting the material with hydrogen. Moreover, the presence of oxygen in films, an element known as an „activator“ for Er ions, doesn't influence also noticeably the films luminescence (see Table 2).

One can assume that the luminescence of Er ions in „amorphous“ samples is activated by the nanocrystals with very small grain sizes ($< 3 \text{ nm}$). The first indication for the presence of these nanocrystals in films has been obtained by the spectroscopic ellipsometry studies. SE data predict the presence of small nanocrystals in samples Er28 and Er33 in amount of 10 and 38%, respectively (SE analysis of the nc-Si thin films with the small nanocrystal grain sizes were discussed in details in [14], see also the models in Fig. 4, b). Indeed, this prediction can be confirmed by HRTEM measurements. A cross-sectional HRTEM image obtains for the sample Er33 is presented in Fig. 4, a). The micrograph shows that the a-Si:H films matrix contains a high density of small clusters that have been identified, on the basis of the electron diffraction analysis, as the silicon nanocrystals. The lattice fringes corresponding to the (111)

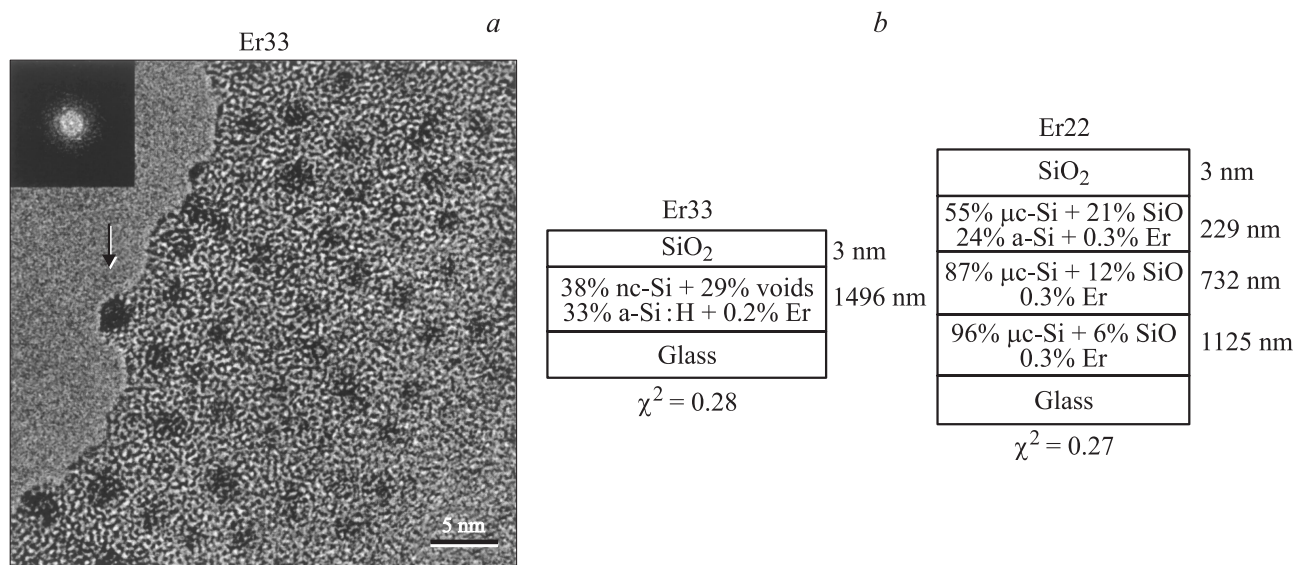


Рис. 4. HRTEM image obtained for the sample Er33 (a) and structural models of the samples Er33 and Er22 derived from SE analysis (b).

planes of silicon are visible in the figure. Statistical analysis of the nanocrystallites size distribution gives the nanocrystal mean radius of about 1.5 nm for this sample. Note, the PL response in the visible range at around 700–720 nm has been also detected in these samples. We believe that in our case the situation is similar to that observed by M. Fujii et al. [15], who has studied the correlation between Er-related PL intensity and the nc-Si grain sizes in nc-Si containing SiO₂ films doped with Er. These authors have obtained the strong, by about two orders of magnitude, increase of Er PL intensity with the lowering of nc-Si grain sizes from 3.8 to 2.7 nm. Actually, starting with these sizes one can speak about the remarkable bandgap widening and the role of quantum size effects in Si [16]. Therefore one can conclude that the seeming strange increase of PL intensity in our „amorphous samples“ can be also understood as a result of sensitizing effect of Si nanocrystals on Er ions that in related with the enhancement of the excitation probability for the last ones due to the recombination of electron-hole pairs confines in nanocrystals.

4. Summary

In this contribution we have shown the ability to produce by the reactive magnetron sputtering method effectively emitting nc-Si:H thin films doped with Er and have discussed their luminescent and structural properties. The nc-Si:Er films with the well-defined crystallinity and nanocrystal sizes (varied from 1–3 to 8 nm) were deposited and studied in both near IR and visible luminescence ranges. The strong influence of Si nanocrystals on the films luminescent properties at 1.54 μm has been observed, where the most intense Er photoluminescence obtained relates to the low crystalline films with the nanocrystal grain sizes less than 3 nm. These films demonstrated intense 1.54 μm luminescence at room temperature with the temperature quenching coefficient (in the range 77–300 K) only of about 5. The results have been explained in terms of the sensitization effect of Si nanocrystals on Er rare-earth ions.

References

- [1] Silicon-Based Optoelectronics / Ed. by S. Coffa, L. Tsybeskov. MRS Bulletin, Iss. 23, 16 (1998).
- [2] J. Stimmer, A. Reittinger, J.F. Nützel, G. Abstreiter, H. Holzbrecher, Ch. Buchal. Appl. Phys. Lett. **68**, 3290 (1996).
- [3] B. Andreev, V. Chalkov, O. Gusev, A. Emel'yanov, Z. Krasil'nik, V. Kuznetsov, P. Pak, V. Shabanov, V. Shengurov, V. Shmagin, N. Sobolev, M. Stepikhova, S. Svetlov. Nanotechnology **13**, 97 (2002).
- [4] P.G. Kik, A. Polman. Mat. Sci. & Eng. B **81**, 1–3, 3 (2001).
- [5] F. Priolo, G. Franzo, F. Iacona, D. Pacifici, V. Vinciguerra. Mat. Sci. & Eng. B **81**, 1–3, 9 (2001).
- [6] M.F. Cerqueira, J.A. Ferreira, G.J. Adriaenssens. Thin Solid Films **370**, 128 (2000).
- [7] M.F. Cerqueira, M. Andritschky, L. Rebouta, J.A. Ferreira, M.F. da Silva. Vacuum **46**, 1385 (1995).
- [8] M. Losurdo, M.F. Cerqueira, E. Alves, M.V. Stepikhova, M.M. Giangregorio, G. Bruno. Physica E **16**, 414 (2003).
- [9] R. Swanepoel. J. Phys. E **16**, 1214 (1998).
- [10] I.H. Campbell, P.M. Fauchet. Solid State Commun. **58**, 739 (1986).
- [11] M. Stepikhova, W. Jantsch, G. Kocher, L. Palmetshofer, M. Schoisswohl, H.J. von Bardeleben. Appl. Phys. Lett. **71**, 2975 (1997).
- [12] G.N. van Hoven, J.H. Shin, A. Polman, S. Lombardo, S.U. Campisano. J. Appl. Phys. **78**, 2642 (1995).
- [13] G. Franzo, V. Vinciguerra, F. Priolo. Appl. Phys. A **69**, 3 (1999).
- [14] M. Losurdo, M.M. Giangregorio, P. Capezzuto, G. Bruno, M.F. Cerqueira, M. Stepikhova, E. Alves. Appl. Phys. Lett. (2003), in print.
- [15] M. Fujii, M. Yoshida, S. Hayashi, K. Yamamoto. J. Appl. Phys. **84**, 4525 (1998).
- [16] T. Takagahara, K. Takeda. Phys. Rev. B **46**, 23, 15 578 (1992).